

Endocytosis of GluN2B-containing NMDA receptor mediates NMDA-induced excitotoxicity

Yu Wu¹, Changwan Chen¹, Qian Yang¹, Mingfei Jiao¹ and Shuang Qiu¹

Abstract

N-methyl-D-aspartate (NMDA) receptor overactivation is involved in neuronal damage after stroke. However, the mechanism underlying NMDA receptor-mediated excitotoxicity remains unclear. In this study, we confirmed that excessive activation of NMDARs led to cell apoptosis in PC12 cells and in primary cultured cortical neurons, which was mediated predominantly by the GluN2B-containing, but not the GluN2A-containing NMDARs. In addition, Clathrin-dependent endocytosis participated in NMDA-induced excitotoxicity. Furthermore, we identified that GluN2B-containing NMDARs underwent endocytosis during excessive NMDA treatment. Peptides specifically disrupting the interaction between GluN2B and AP-2 complex not only blocked endocytosis of GluN2B induced by NMDA treatment but also abolished NMDA-induced excitotoxicity. These results demonstrate that Clathrin-dependent endocytosis of GluN2B-containing NMDARs is critical to NMDA-induced excitotoxicity in PC12 cells and in primary cultured cortical neurons, and therefore provide a novel target for blocking NMDAR-mediated excitotoxicity.

Keywords

N-methyl-D-aspartate receptors, GluN2B, excitotoxicity, endocytosis, oxygen-glutamate deprivation

Date received: 11 January 2017; revised: 22 February 2017; accepted: 2 March 2017

Introduction

N-methyl-D-aspartate receptors (NMDARs) are a subtype of ionotropic glutamate receptors, which play a vital role in the neuronal physiology and pathophysiology.^{1–5} Physiological NMDAR activity is required for neurological functions including synaptic plasticity, memory, and learning. In contrast, excessive activation of NMDAR is thought to mediate the calcium-dependent neurotoxicity that contributes to hypoxic-ischemic brain injury, epilepsy, stroke, and other neuronal diseases. By now, different hypotheses have been put forward as how NMDAR mediates so many different functions. One is the NMDAR location hypothesis that synaptic NMDARs might be coupled to neuroprotective signaling proteins, while extrasynaptic NMDARs to neurodestructive signaling proteins. For example, synaptic NMDARs activate the downstream cyclic-AMP response element-binding protein (CREB) signaling pathway, whereas extrasynaptic NMDARs attenuate the CREB pathway. Another is the NMDAR subtype

hypothesis that different NMDAR subtypes exert distinct effects. NMDARs are heterotetrameric assemblies of two GluN1 subunits and two GluN2 subunits (mostly GluN2A or GluN2B).^{6–8} Activation of GluN2A-containing NMDARs (GluN2A-NMDARs) is linked to several survival-signaling pathways mediated by CREB, Phosphatidylinositol-3 Kinase (PI3K), and Kidins220. In contrast, activation of GluN2B-containing NMDARs (GluN2B-NMDARs) may phosphorylate phosphatase and tensin homolog deleted on

¹Department of Neurobiology, Key Laboratory of Medical Neurobiology (Ministry of Health of China), Collaborative Innovation Center for Brain Science, Zhejiang University School of Medicine, Hangzhou, Zhejiang, China

Corresponding author:

Shuang Qiu, Department of Neurobiology, Key Laboratory of Medical Neurobiology (Ministry of Health of China), Zhejiang University School of Medicine, Hangzhou, Zhejiang 310058, China.
Email: qiuhsly@zju.edu.cn



chromosome 10 (PTEN) to subsequently dephosphorylate Akt and BAD, which result in the deactivation of Akt survival pathway and promote neuronal apoptosis.⁹

Interestingly, several studies have reported that the process of endocytosis is critical for NMDAR-mediated excitotoxicity. Excessive activation of NMDAR results in enhanced endocytosis in organotypic hippocampal cultures.¹⁰ In *Drosophila*, apoptosis induced by overactivation of NMDAR can be inhibited by Dynamin which may block the Clathrin-mediated endocytosis.^{11,12} Furthermore, endocytosis of alpha-Amino-3-hydroxy-5-methylisoxazole-4- propionic acid receptors (AMPA) triggered by overactivation of NMDARs may be an important step involved in NMDAR-mediated excitotoxic neuronal death.^{13–15} In this study, we used integrative experimental approaches and demonstrated that NMDAR-mediated excitotoxicity or oxygen-glutamate deprivation (OGD) in PC12 cells and in primary cultured cortical neurons was mainly dependent on the activation of GluN2B-NMDARs. Moreover, we found that NMDAR-mediated excitotoxicity induced Clathrin-dependent endocytosis of GluN2B-NMDARs. Peptide specifically interrupting the interaction of GluN2B with AP-2 blocked endocytosis of GluN2B-NMDARs and inhibited NMDA-induced excitotoxicity. These findings provide further evidence indicating that GluN2B-NMDARs are critical in NMDAR-mediated excitotoxicity.

Methods

Cell culture and transfection

PC12 cells were a generous gift from Dr Shumin Duan. The cells were maintained in DMEM (Dulbecco modified Eagle medium) plus with 10% Fetal bovine serum (FBS), 100 U/mL Penicillin/streptomycin at 37°C in 5% CO₂ incubator. For Immunocytochemistry (ICC), cells were plated onto poly-L-lysine coated coverslips at a density of 2000 cells/cm². siRNA or plasmids were transfected using Lipofectamine 3000 following the manufacturer's instructions. The final concentration of siRNA duplexes was 20 μM. Cortical tissues were harvested from embryonic day 17 (E17) rats. Cells were digested in 0.25% trypsin/EDTA for 17 min at 37°C, and plated in 35 mm dishes with poly-L-lysine (Sigma) in Neurobasal medium containing 2% B27, 0.5 mM GlutaMAX-I, and 0.5% Fetal bovine serum at 37°C under 5% CO₂. After 4h, the medium was replaced with neurobasal medium supplemented with 2% SM1 (Stem Cell), 0.5 mM GlutaMAX-I, 100 IU/ml penicillin, and 100 μg/ml streptomycin sulfates. Subsequently, the culture medium was replaced every five days. At three days in vitro (DIV 3), Cytosine D-Aarbino-Furanoside (Sigma) was added at a final concentration of 5 μM.

Reagents, antibodies, and plasmids

MK-801, poly-L-lysine, NMDA, D-APV, ifenprodil, chlorpromazine, ZnCl₂, and DAPI nuclear dye were purchased from Sigma Aldrich. Dynasore and CGP-78608 were purchased from Tocris Bioscience. Antibodies against PSD95, ^{Y1472}P-GluN2B, ^{Y1070}P-GluN2B, β-actin, and Clathrin light chain were obtained from Abcam. Cleaved Caspase 3 was purchased from Cell Signaling Technology. Antibody against GluN2B mAb was made as described previously.¹⁶ Peptides: Scramble (YGRKKRRQRRRNGHVAEKLSSIE), Tat-YEKL (YGRKKRRQRRRNGHVYEKL SSIE), and Dynamin inhibitor peptide (Myr-4-QVPSRPNRAP) were synthesized by GL Biochem (Shanghai, China). Clathrin siRNA (GUAGUCUCCUAUUUUCAUAC) and control siRNA were synthesized by GenePharma (Shanghai, China). Protein A Sepharose beads were purchased from GE Healthcare. Horseradish peroxidase-linked goat anti-mouse immunoglobulin G (IgG) and goat anti-rabbit IgG, secondary antibodies conjugated to Dylight (555), and chemiluminescence kit were purchased from Thermo Fisher. Rab5_{WT}-GFP and Rab5_{S34N}-GFP were gifts from Yiting Zhou.

Cell viability assay

The viability of cells was measured using CCK8 (Dojindo) assays. In brief, PC12 cells were seeded in 96-well at a concentration of 5000 per well. After treatment, the medium was added with 10 μl CCK8 agent solution, then cells were incubated for another 3 h at 37°C in the dark. Absorbance at 450 nm was measured with a microplate reader (iMark, Bio-Rad) and the results were normalized to untreated cells.

Annexin and propidium iodide assay

Apoptotic cells were measured using Annexin V/PI (Roche) assay. In brief, cells were washed with ice-cold phosphate buffer saline (PBS) and resuspended in binding buffer. The cell suspension was transferred into a tube and double-stained with Annexin V-FITC and propidium iodide (PI) at room temperature in the dark for 15 min, according to the instructions of the manufacturer. The apoptotic cells were detected by fluorescence microscopy (FV1000, Olympus). DAPI staining was performed according to the instruction with the kit (Beyotime Biotech).

Immunostaining

Cells were fixed at room temperature with 4% paraformaldehyde in PBS for 15 min, permeabilized with 0.2%

Triton X-100 (Amresco) in PBS, and then blocked for 30 min in blocking solution containing 2.5% BSA fraction V (Amresco) in PBS. In the following, cells were incubated in primary antibody for 1 h at room temperature and then incubated with secondary antibody in blocking solution for another 1 h at room temperature. After being washed, cells were mounted with ProLongGold (Molecular Probes).

Oxygen-glucose deprivation

Cells were rinsed twice with PBS and incubated in glucose-free DMEM. In the following, cells were introduced into an anaerobic chamber containing a mixture of 95% N₂ and 5% CO₂ at 37°C for 4 h. After oxygen glucose deprivation, cells were washed with glucose containing DMEM for three times and then maintained in glucose-containing DMEM at 37°C in a humidified 5% CO₂ incubator for indicated times to imitate the process of reperfusion.

Surface biotinylation

Cells were rinsed twice with ice-cold PBS containing 0.1 mM CaCl₂ and 1 mM MgCl₂ (Buffer A), and then incubated with 0.25 mg/ml Sulfo-NHS-SS-biotin (Pierce) in Buffer A for 20 min at 4°C. After incubated in Buffer A containing 20 mM glycine for 5 min at 4°C, the neurons were lysed in Buffer B (10 mM Tris (pH 7.4), 150 mM NaCl, 1 mM EDTA, 0.1% SDS, 1% Triton X-100, and 1% sodium deoxycholate) supplemented with protease and phosphatase inhibitors, and then centrifuged at 12,000 g for 15 min at 4°C. Supernatant were incubated overnight with NeutrAvidin beads (Pierce) at 4°C. Beads were washed four times with radio-immunoprecipitation (RIPA) buffer and twice with PBS, and then protein was resolved by SDS-gel and subjected to Western blot analysis.

Co-immunoprecipitation

Co-immunoprecipitation (Co-IP) was carried out as reported previously.¹⁷ Briefly, neurons were lysed in a RIPA assay buffer (50 mM Tris-HCl (pH 7.4), 150 mM NaCl, 1% NP-40, 0.25% sodium deoxycholate, 2 mM EDTA, 0.1 mM PMSF), supplemented with phosphatase inhibitor cocktails 2 and 3. After centrifuged (12,000 g, at 4°C) for 30 min, the pellet was discarded, and the supernatant was preincubated with IP antibody or IgG overnight at 4°C. Protein A-Sepharose was then added and incubated for another 2 h at 4°C. The mixtures were washed three times with RIPA assay buffer, eluted by boiling in 2 × Laemmli buffer, and subjected to Western blot analysis with the antibodies accordingly.

Western blot

Western blot was conducted as described previously.¹⁸ Protein samples were performed on SDS-polyacrylamide gels and separated proteins was transferred to nitrocellulose membrane (Whatman, GE Healthcare). The membranes were blocked with 5% BSA in Tris-buffered saline with Tween-20 (TBST) at room temperature for 2 h and were incubated with primary antibodies overnight at 4°C. After being washed for three times with TBST, the membranes were incubated with appropriate horseradish peroxidase-linked secondary antibody (1:10000) for 1 h at room temperature, followed by detection of the proteins with the chemiluminescence reagent according to the instructions of the manufacturer. The density of the Western blot was measured with Quantity One under GS-800 Calibrated Densitometer (Bio-Rad).

Statistical analyses

All data are shown as the mean ± the standard error of the mean (SEM). Differences between two groups were tested by unpaired, two-tailed Student's *t*-test or Mann-Whitney rank sum test, based on a normality test (Shapiro-Wilk). For comparison of more than two groups, one-way analysis of variance (ANOVA) and a Bonferroni's test for multiple comparison post hoc tests were used. Statistical analysis was carried out using Prism 5 software (GraphPad). Significance was indicated as #### or ***P < 0.005; ## or **P < 0.01; # or *P < 0.05.

Results

NMDA- and OGD-induced toxicity in PC12 cells

Sustained activation of NMDARs leads to excitotoxic neuronal death in stroke, trauma, and neurodegenerative diseases.^{19,20} In this study, PC12 cells were incubated with different concentrations of NMDA (20, 50, 100, 250, 500, and 1000 μM) for 24 h. Consistent with previous studies, we found that high concentration of NMDA (250, 500, and 1000 μM) leads to decreased cell viability analyzed by CCK8 assay (Figure 1(a)). About 50% PC12 cells died after bath applied with 500 μM NMDA for 24 h, whereas less than 20% of cells died after applied with 100 μM NMDA (Figure 1(a)). Moreover, NMDA-induced excitotoxicity in PC12 cells exhibited a time-dependent manner when incubation with 500 μM NMDA for a variety of time periods (2, 6, 12, 24, 48, or 72 h) (Figure 1(b)). Cell death was significantly increased after exposure with 500 μM NMDA for 12 h or longer. To further investigate whether NMDA-induced cell death was programmed in PC12 cells, cleaved Caspase 3 was detected by Western blot at

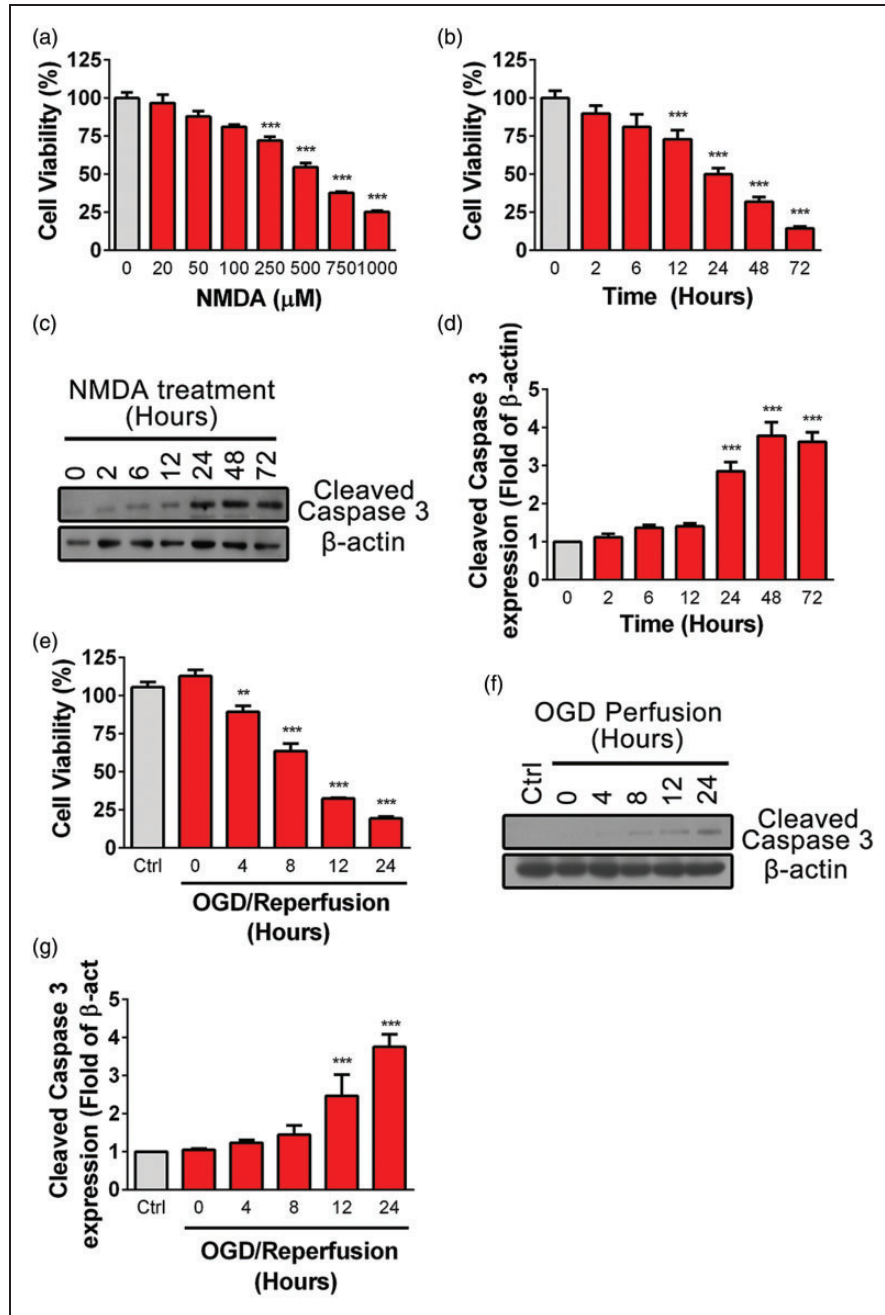


Figure 1. Excessive NMDA treatment or OGD induces PC12 cell death. (a) PC12 cells were treated with NMDA at different concentrations (0, 20, 50, 100, 200, 500, 750, 1000 μ M) for 24 h in serum free media (SFM) and cell viability was assayed by CCK8, ***P < 0.005 compare to control. (b) PC12 cells were treated with NMDA (500 μ M in SFM) for different time periods (0, 2, 6, 12, 24, 48, 72 h) and cell viability was assayed by CCK8, ***P < 0.005 compare to control. (c and d) PC12 cells were treated with NMDA (500 μ M in SFM) for different time point (0, 2, 6, 12, 24, 48, 72 h), the abundance of cleaved Caspase 3 were detected by Western blot. The cleaved Caspase 3/ β -actin ratios were plotted as average \pm SEM (n = 3), ***P < 0.005 compare to control. (e) PC12 cells were exposed to OGD (4 h) followed by reperfusion for various periods (0, 4, 8, 12, 24 h) and cell viability was assayed by CCK8, **P < 0.01, ***P < 0.005 compare to control. (f and g) PC12 cells were exposed to OGD (4 h) followed by reperfusion for different periods (0, 4, 8, 12, 24 h) and the abundance of cleaved Caspase 3 was determined by Western blot. The cleaved Caspase 3/ β -actin ratios were plotted as average \pm SEM (n = 3), ***P < 0.005 compare to control.

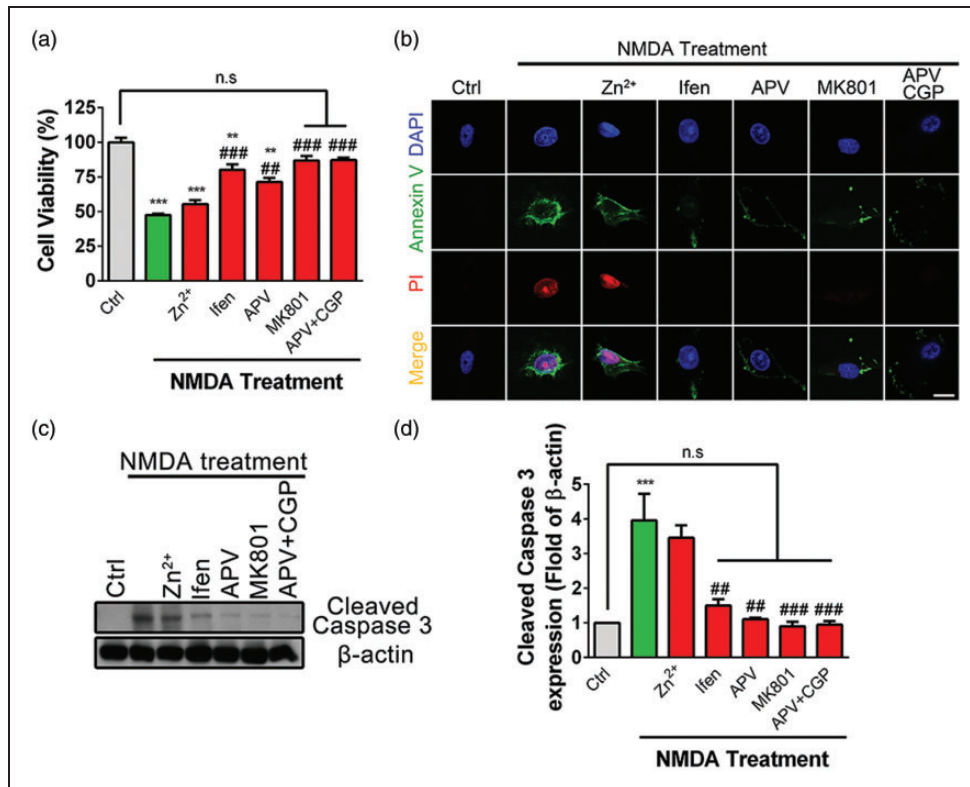


Figure 2. GluN2B-NMDARs mediate excitotoxicity induced by excessive NMDA treatment in PC12 cells. (a) PC12 cells were pretreated with Zn²⁺ (100 nM), ifenprodil (Ifen, 10 μM), APV (100 μM), MK801 (10 μM), or APV (100 μM) + CGP-78608 (CGP, 1 μM), for 4 h, separately, followed by stimulation with NMDA (500 μM) for 24 h in SFM. Cell viability was assayed by CCK8, **P < 0.01, ***P < 0.005 compare to control, ###P < 0.01, ####P < 0.005 compared to NMDA treatment, n.s.: not significant. (b) PC12 cells were pretreated with Zn²⁺ (100 nM), Ifen (10 μM), APV (100 μM), MK801 (10 μM), or APV (100 μM) + CGP (1 μM) for 4 h, separately, followed by stimulation with NMDA (500 μM) for 24 h in SFM. Cells were immunostained with Annexin V (green), PI (red), and DAPI (Blue), and then evaluated for apoptosis. (c and d) PC12 cells were pretreated with Zn²⁺ (100 nM), Ifen (10 μM), APV (100 μM), MK801 (10 μM), or APV (100 μM) + CGP (1 μM) for 4 h, separately, followed by stimulation with NMDA (500 μM) for 24 h in SFM. The abundance of cleaved Caspase 3 was determined by Western blot. The cleaved Caspase 3/β-actin ratios were plotted as average ± SEM (n = 3), ***P < 0.005 compare to control, ###P < 0.01, ####P < 0.005 compared to NMDA treatment, n.s.: not significant.

various time points (2, 6, 12, 24, 48, or 72 h) after treatment with 500 μM NMDA. The result showed that cleaved Caspase 3 was significantly increased after incubation with NMDA for 24 h (Figure 1(c) and (d)).

Next, an in vitro ischemia-like OGD model was used to induce delayed cell death as occurring in vivo.^{21,22} PC12 cells were subject to OGD for 4 h at 37°C followed by reperfusion (OGD/R) for various time (4, 8, 12, or 24 h). As shown in Figure 1(e), OGD for 4 h did not affect cell viability, while reperfusion for 4 h after OGD significantly decreased. Additionally, cleaved Caspase 3 was significantly increased after reperfusion for 12 h (Figure 1(f) and (g)). These data were in consistent with previous finding that excessive NMDA treatment or OGD/R induces programmed cell death.

Activation of GluN2B-NMDAR subtype is responsible for NMDA-induced excitotoxicity

Previous studies suggest that different NMDAR subtypes have differential roles in excitotoxic neuronal death.^{15,23,24} Here, we investigated whether specific subtype of NMDARs was involved in NMDA-mediated excitotoxicity in PC12 cells (Figure 2(a)). Pharmacological pore block with MK801 completely abolished NMDA-induced cell death, whereas competitive NMDAR antagonist APV significantly, but not completely blocked NMDA-induced cell death. In addition, several recent studies suggest that NMDARs have not only ionotropic but also metabotropic function,^{25–28} which may participate in NMDA-mediated

excitotoxicity.²⁵ In the following, APV and CGP-78608 (CGP) were bath applied to block ligand binding sites of glutamate and D-serine to effectively block the metabotropic functions of NMDARs. Bath application of APV + CGP completely abolished NMDA-induced cell apoptosis, indicating that metabotropic signaling of NMDARs is also involved in NMDA-mediated excitotoxicity. To further test the role of GluN2A-NMDARs or GluN2B-NMDARs in NMDA-mediated excitotoxicity, PC12 cells were pretreated with low concentration of Zinc (200 nM), which has been reported to specifically block GluN2A-NMDAR^{29,30} or GluN2B-NMDAR antagonist ifenprodil (10 μ M). As shown in Figure 2(a), pretreatment with ifenprodil, but not Zinc, significantly prevented NMDA-induced cell death, indicating that GluN2B-NMDAR plays a dominant role in mediating NMDA-induced excitotoxicity.

Additionally, the fluorescent intensity of Annexin V and PI were significantly increased after incubation with NMDA, whereas pretreatment with MK801 or APV + CGP completely blocked such enhancement and pretreatment with ifenprodil or APV partially and significantly blocked such enhancement (Figure 2(b)). In contrast, pretreatment with Zinc had no effect on NMDA-induced upregulation of the fluorescent intensity of Annexin V or PI. Moreover, NMDA-induced upregulation of the abundance of cleaved Caspase 3 was significantly reduced by pretreatment with APV, MK801, ifenprodil, or APV + CGP, but not by GluN2A antagonist Zinc (Figure 2(c) and (d)).

Clathrin-mediated endocytosis participates in NMDA-induced excitotoxicity in PC12 cells

Previous studies using pharmacological reagents have suggested that endocytosis is involved in NMDA-induced excitotoxicity in cultured neurons.^{15,31,32} Consistently, our results showed that pretreatment with inhibitors of Clathrin-mediated endocytosis, such as Chlorpromazine (CPZ, 15 μ M), non-competitive Dynamin inhibitor Dynasore (80 μ M), or Dynamin inhibitor peptide (DIP, 50 μ M), respectively, significantly inhibited NMDA-induced cell death (Figure 3(a)). Additionally, NMDA-induced upregulation of the fluorescent intensity of Annexin V and PI was abolished when pretreated with DIP, CPZ, or Dynasore (Figure 3(b)). Furthermore, NMDA-induced enhancement of the abundance of cleaved Caspase 3 was attenuated when pretreated with DIP, CPZ, or Dynasore (Figure 3(c) and (d)).

To exclude the non-specific effect of Clathrin-mediated endocytosis inhibitors, Clathrin small interference RNA (siRNA) was transfected into PC12 cells to knock down endogenous Clathrin (Figure 3(e)). NMDA-induced upregulation of cleaved Caspase 3 was

significantly decreased when Clathrin was knocked down compared to the control siRNA (Figure 3(e) and (f)). Rab5 is a key mediator involved in the endocytosis of membrane proteins.³³ Here, we transfected Rab5_{WT}-GFP or its dominant negative mutation Rab5_{S34N}-GFP into PC12 cells and observed that, followed by bath application with 500 μ M NMDA for 24 h, the fluorescent intensity of cleaved Caspase 3 was significantly decreased in cells transfected with Rab5_{S34N}-GFP compared to that transfected with Rab5_{WT}-GFP (Figure 3(g) and (h)). These data confirmed that Clathrin-mediated endocytosis was involved in NMDA-induced excitotoxicity in PC12 cells.

Excessive NMDA treatment induces endocytosis of GluN2B

Our upper results indicate that both activation of GluN2B-NMDARs and Clathrin-mediated endocytosis are critical for NMDA-induced excitotoxicity. Next, we asked whether surface expression of GluN2B-NMDARs is changed during excessive NMDA stimulation. By using surface biotinylation assay, we observed that surface GluN2B was significantly decreased after NMDA treatment (Figure 4(a) and (b)). Previous work has shown that phosphorylation of GluN2B at Tyrosine 1472 site is closely related to the endocytosis of GluN2B-NMDARs. High phosphorylation level of ^{Y1472}P-GluN2B blocks the interaction of GluN2B with AP-2 component of the endocytic machinery and inhibits endocytosis.³⁴ ^{Y1070}P-GluN2B is another tyrosine phosphorylation site of GluN2B that has been reported to be regulated by synaptic activity in the cultured neurons. We then tested the effect of NMDA treatment on the phosphorylation level of ^{Y1472}P-GluN2B or ^{Y1070}P-GluN2B at various time points (2, 6, 12, 24, 48, or 72 h) in PC12 cells. As shown in Figure 4(c)–(e), NMDA incubation for 24 h or longer significantly decreased the phosphorylation level of GluN2B at Y1472 site but not that of Y1070 site. Similarly, the phosphorylation level of GluN2B at Y1472 site was significantly decreased 12 h after OGD reperfusion (Figure 4(f) and (g)), indicating that the endocytosis of GluN2B-NMDARs is increased during NMDA-induced excitotoxicity.

Endocytosis of GluN2B-NMDARs is critical for NMDA-induced excitotoxicity

To test whether endocytosis of GluN2B-NMDARs is involved in NMDA-induced excitotoxicity in PC12 cells, we utilized a cell membrane penetrating peptide Tat-YEKL according to the YEKL motif (Figure 5(a)).³⁵ By using surface biotinylation assay, we found that NMDA-induced endocytosis of GluN2B-NMDARs was completely blocked by pretreatment

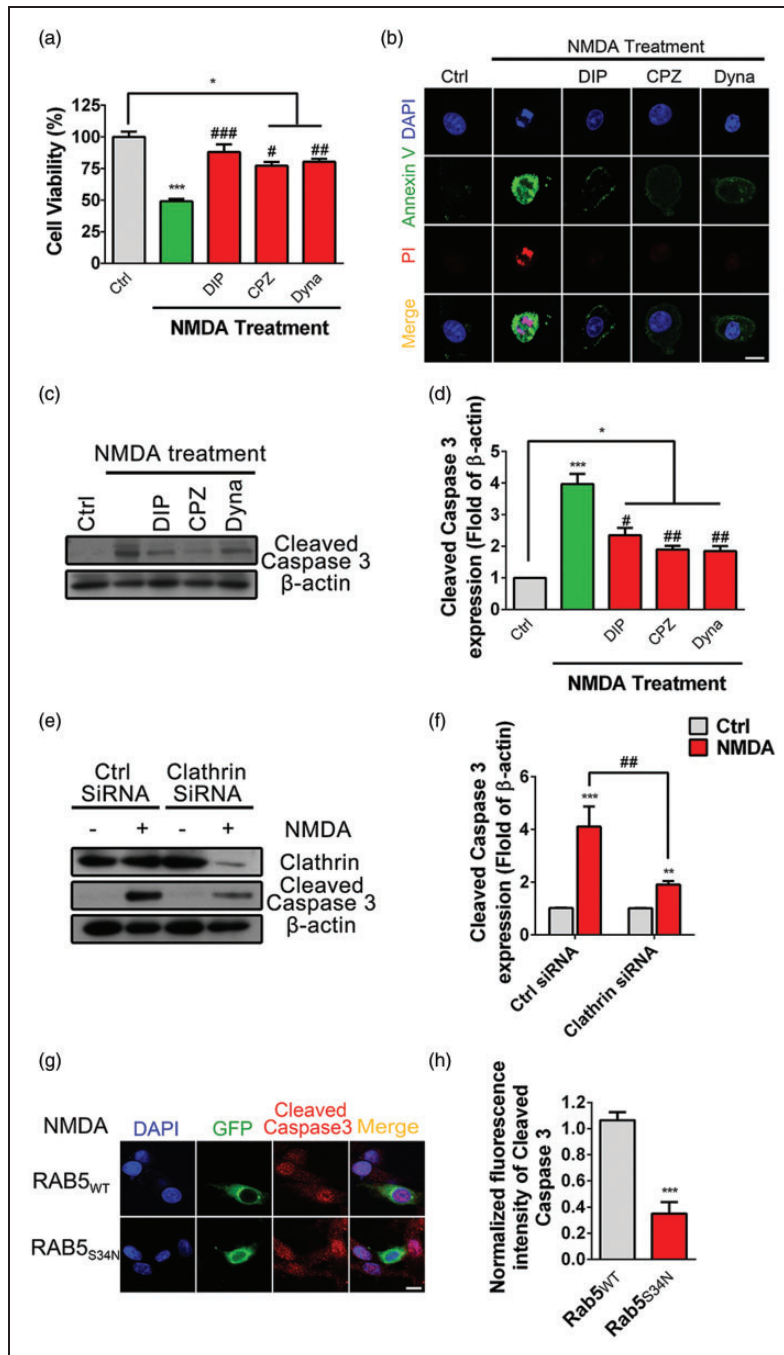


Figure 3. Clathrin-mediated endocytosis participates in NMDA-induced excitotoxicity in PC12 cells. (a) PC12 cells were pretreated with Dynamin inhibit peptide (DIP, 50 μ M), Chlorpromazine (CPZ, 20 μ M) or Dynasore (100 μ M) for 4 h, respectively, followed by stimulation with NMDA (500 μ M) for 24 h, and cell viability was assayed by CCK8, * $P < 0.05$, *** $P < 0.005$ compared to control, # $P < 0.05$, ### $P < 0.01$, #### $P < 0.005$ compared to NMDA treatment. (b) PC12 cells were pretreated with DIP (50 μ M), CPZ (20 μ M), or Dynasore (100 μ M) for 4 h, separately, followed by stimulation with NMDA (500 μ M) for 24 h in SFM, and cells were immunostained with Annexin V (green), PI (red), and DAPI (Blue), and then evaluated for apoptosis. (c and d) PC12 cells were pretreated with DIP (50 μ M), CPZ (20 μ M), or Dynasore (100 μ M) for 4 h, separately, followed by stimulation with NMDA (500 μ M) for 24 h in SFM, the abundance of cleaved Caspase 3 was determined by Western blot. The cleaved Caspase 3/ β -actin ratios were plotted as average \pm SEM ($n = 5$), * $P < 0.05$, *** $P < 0.005$ compared to control, # $P < 0.05$, ### $P < 0.01$ compared to NMDA treatment. (e and f) PC12 cells were transfected with Clathrin siRNA or Control (Ctrl) siRNA. After 48 h, cells were incubated with NMDA (500 μ M) for 24 h in SFM, the abundance of cleaved Caspase 3 was determined by Western blot. The Clathrin siRNA knockdown efficiency was confirmed by antibody against Clathrin light chain. The cleaved Caspase 3/ β -actin ratio was plotted as average \pm SEM ($n = 3$), *** $P < 0.005$ compared to control, ### $P < 0.01$ compared to NMDA treatment. (g and h) PC12 cells were transfected with RAB5_{WT}-GFP or RAB5 dominant negative plasmid RAB5_{S34N}-GFP. After 48 h, cells were incubated with NMDA (500 μ M) for 24 h and cell death was measured by immunostaining with antibodies against cleaved Caspase 3 (red), GFP (green), and with DAPI (blue). The fluorescence intensity of cleaved Caspase 3 were plotted as average \pm SEM, *** $P < 0.005$.

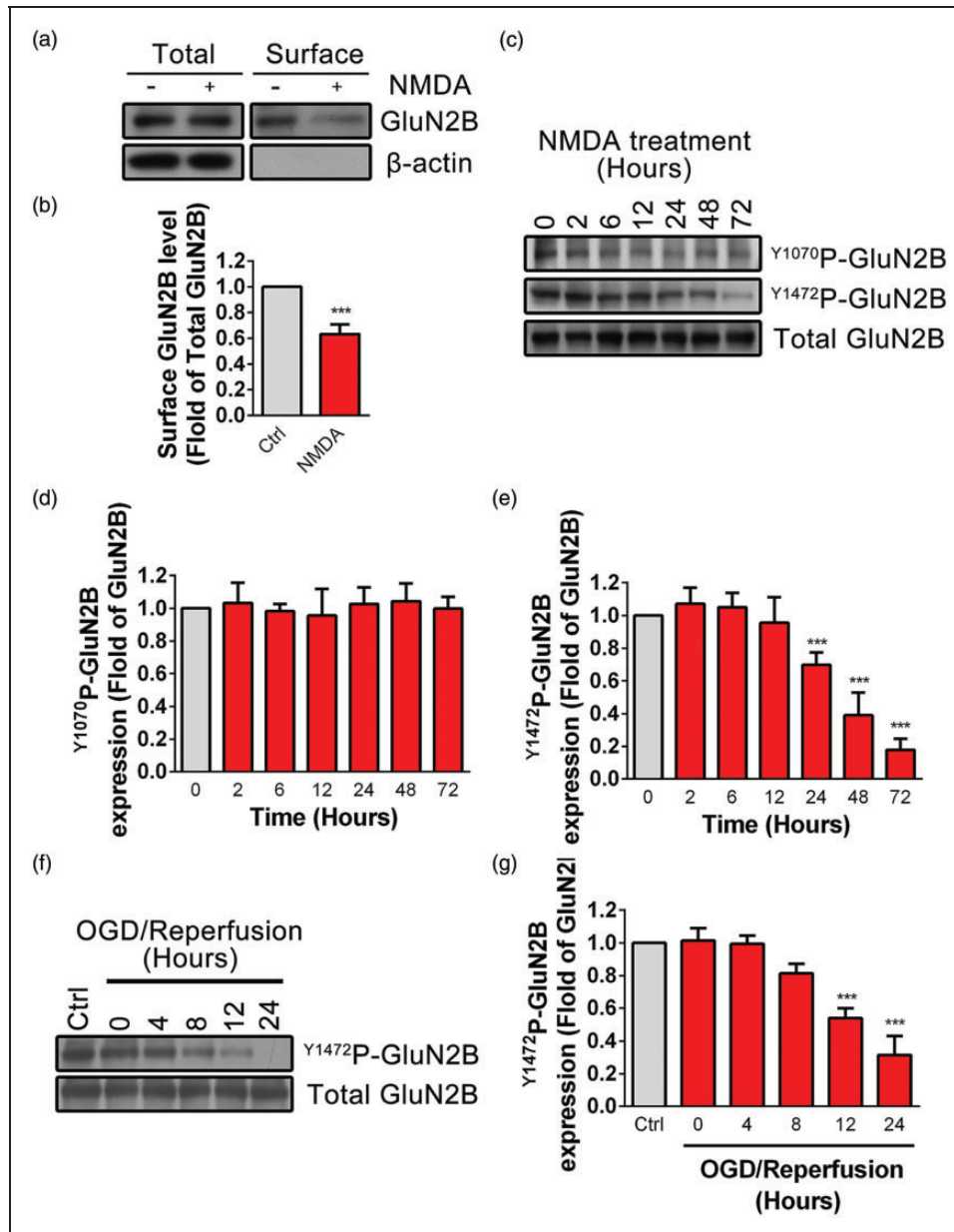


Figure 4. GluN2B undergoes endocytosis and dephosphorylation at the Y1472 site during excessive NMDA treatment or OGD/R in PC12 cells. (a and b) PC12 cells were treated with NMDA (500 μ M in SFM) for 24 h. The surface expression of GluN2B was detected by surface biotinylation assay. β -actin was set as negative control. Surface GluN2B/total GluN2B ratios were plotted as average \pm SEM (n = 5), ***P < 0.005. (c to e) PC12 cells were treated with NMDA (500 μ M in SFM) for different time (0, 2, 6, 12, 24, 48, 72 h) and the phosphorylation level of Y1070 P-GluN2B or Y1472 P-GluN2B was determined by Western blot. The Y1070 P-GluN2B/total GluN2B or Y1472 P-GluN2B/total GluN2B ratios were plotted as average \pm SEM (n = 5), ***P < 0.005 compared to control. (f and g) PC12 cells were exposed to OGD (4 h) followed by reperfusion for different period (0, 4, 8, 12, 24 h). The phosphorylation level of Y1472 P-GluN2B were determined by Western blot. The Y1472 P-GluN2B/Total GluN2B ratios were plotted as average \pm SEM (n = 3), ***P < 0.005 compared to control.

with Tat-YEKL (50 μ M) but not the scramble peptide (SCR, 50 μ M) (Figure 5(b) and (c)). It should be mentioned that Tat-YEKL used here is partly overlapped with previously reported Tat-NR2B9c peptide which could block the interaction of PSD95 with GluN2B and prevent NMDA-induced cell death. Therefore, we examined whether bath application of Tat-YEKL had

any effects on the interaction between GluN2B and PSD95 (Figure 5(d) and (e)). Co-IP assay suggested that both Tat-YEKL and its scramble peptide had no effect on the binding of GluN2B with PSD95. However, pretreatment with Tat-YEKL, but not SCR, significantly blocked NMDA-induced excitotoxicity (Figure 5(f)). Moreover, the enhanced fluorescent

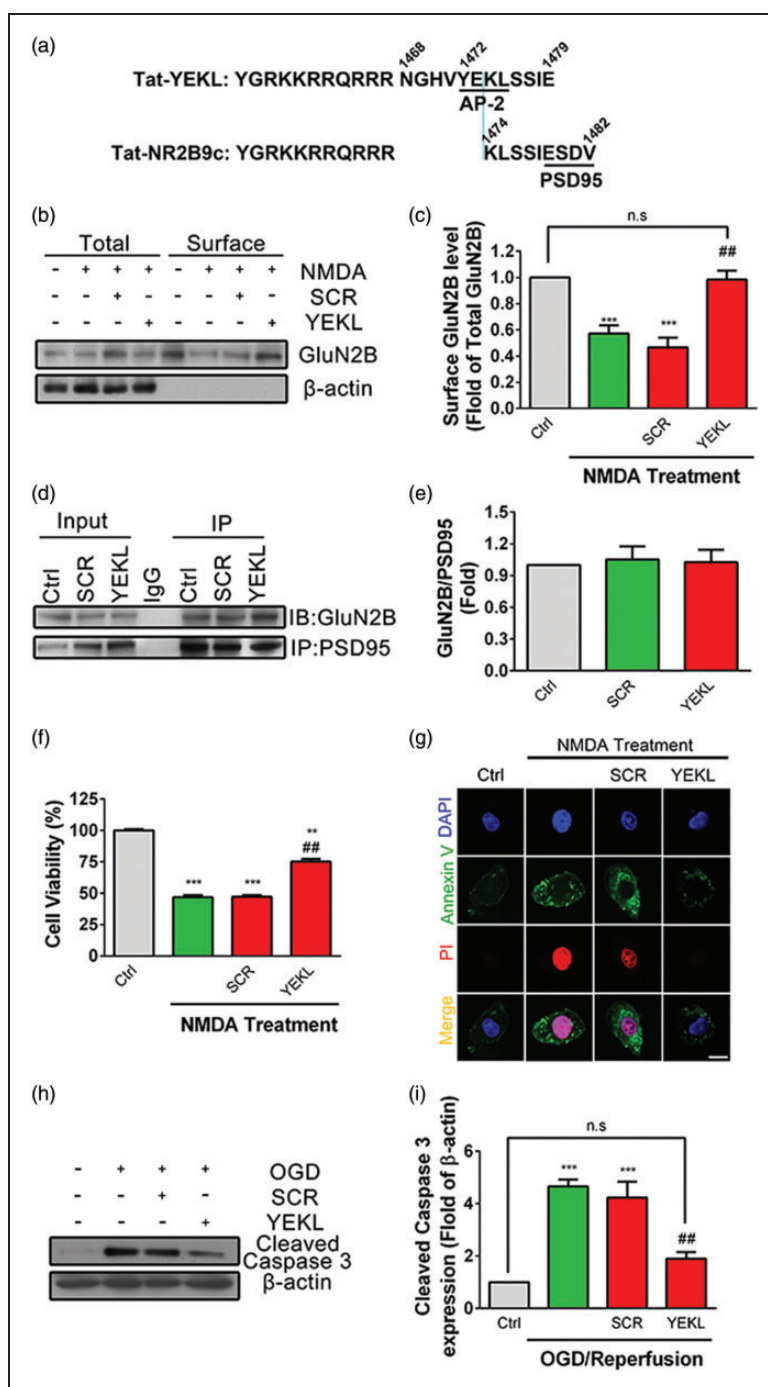


Figure 5. Blocking GluN2B endocytosis with specific peptide attenuates NMDA-induced excitotoxicity in PC12 cells. (a) The amino acid sequence of the Tat-fused YEKL (1468-1479 aa of GluN2B) or NR2B9c (1474-1482 aa of GluN2B) were represented. AP-2 binding motif and PDZ-binding domain were underlined. (b and c) PC12 cells were pretreated with Scramble Peptide (SCR, 50 μ M) or Tat-YEKL (YEKL, 50 μ M) for 4 h, separately, followed by stimulation with NMDA (500 μ M) for 24 h in SFM. Surface expression of GluN2B was detected by surface biotinylation assay. β -actin was set as negative control. Surface GluN2B/total GluN2B ratios were plotted as average \pm SEM ($n = 5$). *** $P < 0.005$ compared to control, ### $P < 0.01$ compared to NMDA treatment. (d and e) PC12 cells were pretreated with SCR (50 μ M) or YEKL (50 μ M) for 4 h, separately, followed by stimulation with NMDA (500 μ M) for 24 h in SFM. The interaction between GluN2B and PSD95 was determined by Co-IP ($n = 5$). (f) PC12 cells were pretreated with SCR (50 μ M) or YEKL (50 μ M) for 4 h, separately, followed by stimulation with NMDA (500 μ M) for 24 h in SFM, and cell viability was assayed by CCK8, *** $P < 0.01$, **** $P < 0.005$ compared to control, ### $P < 0.01$, compared to NMDA treatment. (g) PC12 cells were pretreated with SCR (50 μ M) or YEKL (50 μ M) for 4 h, followed by stimulation with NMDA (500 μ M) for 24 h in SFM, and cells were immunostained with Annexin V (green), PI (red), and DAPI (Blue) and then evaluated for apoptosis. (h and i) PC12 cells were pretreated with SCR (50 μ M) or YEKL (50 μ M) for 4 h, separately, followed by exposure to OGD (4 h) and reperfusion (24 h), and the abundance of cleaved Caspase 3 was determined by Western blot. The cleaved Caspase 3/ β -actin ratios were plotted as average \pm SEM ($n = 3$), *** $P < 0.005$ compared to control, ### $P < 0.01$ compared to NMDA treatment, n.s.: not significant.

intensity of Avnnexin V and PI induced by NMDA was significantly reduced when pretreated with YEKL but not with SCR peptide (Figure 5(g)). NMDA-induced upregulation of cleaved Caspase 3 was significantly inhibited by pretreatment with Tat-YEKL, but not SCR peptide (Figure 5(h) and (i)). These data suggest that endocytosis of GluN2B-NMDARs is involved in NMDA-induced excitotoxicity.

Clathrin-mediated endocytosis participates in NMDA-induced excitotoxicity in primary cultured neurons

To test whether clathrin-mediated endocytosis participates in NMDA-induced excitotoxicity in primary cultured neurons, we detected the effect of NMDA (100 μ M) treatment on the phosphorylation level of 32 P-GluN2B at various time points (1, 3, 6 h) in the cultured cortical neurons. As shown in Figure 6(a) and (b), NMDA incubation for 3 h or longer significantly decreased the phosphorylation level of GluN2B at Y1472 site. We further assessed whether NMDA-induced apoptosis could be abolished when the cultured cortical neurons were pretreated with inhibitors of Clathrin-mediated endocytosis. By staining assay, we observed that NMDA-induced DNA fragmentation of nuclei was significantly decreased when pretreated with DIP, CPZ, or Dynasore followed by treatment with NMDA (100 μ M) for 3 h (Figure 6(c) and (d)). Furthermore, NMDA-induced enhancement of the abundance of cleaved Caspase 3 was attenuated when pretreated with DIP, CPZ, or Dynasore (Figure 6(e) and (f)). Finally, we pretreated the neurons with peptide YEKL and its scramble peptide. As shown in Figure 6(g) and (h), pretreatment with YEKL, but not its scramble peptide, significantly prevented NMDA-induced neuronal death. Moreover, NMDA-induced upregulation of cleaved Caspase 3 was significantly inhibited by pretreatment with YEKL, but not scramble peptide (Figure 6(i) and (j)). These data suggest that endocytosis of GluN2B-NMDARs is involved in NMDA-induced excitotoxicity in primary cultured neurons.

Discussion

In the present study, we have confirmed that NMDA induces dose- and time-dependent excitotoxicity and time-dependent OGD/reperfusion process in PC12 cells. In addition, GluN2B-NMDAR plays a dominant role in mediating NMDA-induced cell death. Furthermore, Clathrin-mediated endocytosis is also critical in triggering excitotoxicity induced by excessive treatment with NMDA. More importantly, we observed the endocytosis of GluN2B-NMDARs during NMDA treatment, and blocking the endocytosis of GluN2B-

NMDARs with peptide significantly inhibits NMDA-induced cell death.

Previous researches have indicated that the GluN2B subunit is a major hub for NMDA-induced excitotoxicity. The GluN2B/PSD95/nNOS complex is a well-established pathway that participates in neuronal cell death. PSD95 binds to the C terminal PDZ domain of GluN2B and recruits nNOS to the NMDARs to mediate the production of the nitric oxide.^{36–38} Moreover, GluN2B interacts with death-associated protein kinase 1, which allows death-associated protein kinase 1 to specifically potentiate GluN2B function and thereby activate the receptor-mediated death signaling. Recruitment of PTEN to GluN2B is another possible mechanism that potentiates GluN2B channel activity and contributes to GluN2B-mediated neuronal death following stroke. Here, our results confirmed that GluN2B-NMDAR is critical for NMDA-induced excitotoxicity, in consistent with previous findings. Additionally, we provide the first evidence that endocytosis of GluN2B itself participates in GluN2B-mediated death signaling. We showed that overactivation of NMDARs induced endocytosis of the GluN2B subunit (Figure 4(a)). Moreover, the phosphorylation level of GluN2B at Y1472 site, a critical site for blocking the endocytosis of GluN2B, is decreased during NMDA stimulation, indicating that the endocytosis of GluN2B is increased. Most importantly, peptide specifically blocking the interaction of GluN2B and AP-2 is able to reverse NMDA-induced excitotoxicity. Therefore, our results provide consolidate evidence indicating that endocytosis of GluN2B is another important mechanism for NMDAR-mediated cell death. It should be mentioned that these treatment could not completely block excitotoxicity, which means that other cellular process may also participate in NMDAR activation-induced excitotoxicity. Taken together, our results indicate that GluN2B-NMDAR endocytosis is one of the key pathways mediating the excitotoxicity of NMDA overstimulation. When endocytosis is blocked, activation of surface NMDARs may not effectively lead to excitotoxicity. In consistent with our finding, one of the previous researches has shown that the calcium chelator EGTA totally blocked NMDA-induced endocytosis, indicating the dependence of endocytosis on calcium entry through NMDARs.³¹ Moreover, NMDA-induced neuronal death was prevented by broad spectrum inhibitors of clathrin-mediated endocytosis, demonstrating that the process of endocytosis is critical for NMDA-induced excitotoxicity.²⁴

Previous work has reported a peptide (Tat-NR2B9c) designed according to the C terminal 9 amino acids of GluN2B to block the interaction of PSD95 and GluN2B, which in turn abolishes the association of nNOS with GluN2B and prevents NMDA-induced cell death (Figure 5(a)). In contrast, our peptide is designed

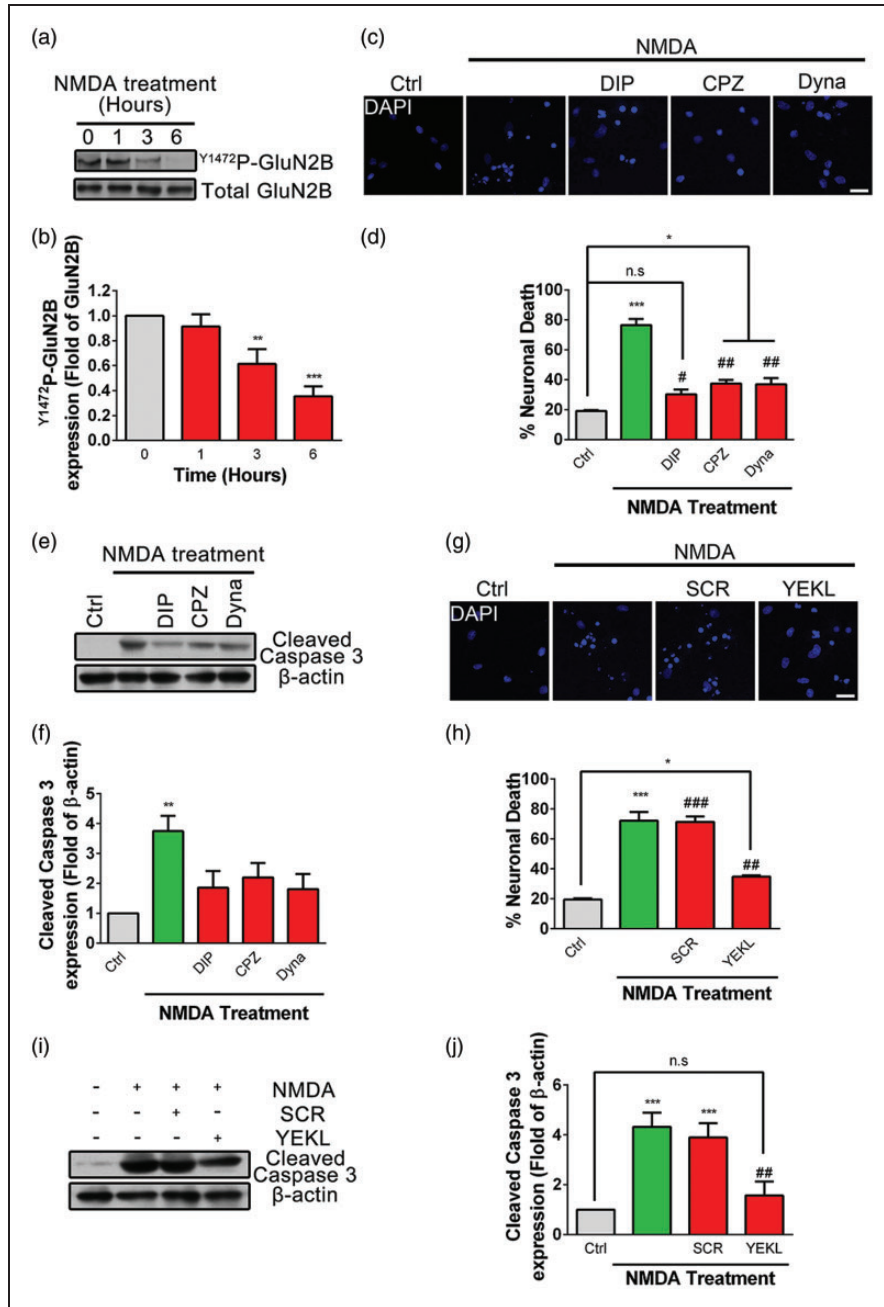


Figure 6. Blocking GluN2B endocytosis with peptide YEKL attenuates NMDA-induced excitotoxicity in cultured cortical neurons. (a and b) Cortical neurons at DIV 10-11 were treated with NMDA (100 μM) for different time (0, 1, 3, 6 h) and the phosphorylation level of Y¹⁴⁷²P-GluN2B was determined by Western blot. The Y¹⁴⁷²P-GluN2B/total GluN2B ratios were plotted as average ± SEM (n = 3), **P < 0.01, ***P < 0.005 compared to control. (c and d) Cortical neurons at DIV 10-11 were pretreated with DIP (50 μM), CPZ (20 μM), or Dynasore (100 μM) for 1 h, separately, followed by stimulation with NMDA (100 μM) for 3 h, and cells were stained with DAPI (Blue). The neuronal death ratios were plotted as average ± SEM (n = 3), *P < 0.05, ***P < 0.005 compared to control, #P < 0.05, ###P < 0.01 compared to NMDA treatment. (e and f) Cortical neurons at DIV 10-11 were pretreated with DIP (50 μM), CPZ (20 μM), or Dynasore (100 μM) for 1 h, separately, followed by stimulation with NMDA (100 μM) for 3 h, the abundance of cleaved Caspase 3 was determined by Western blot. The cleaved Caspase 3/β-actin ratios were plotted as average ± SEM (n = 3), **P < 0.01 compared to control. (g and h) Cortical neurons were pretreated with YEKL (50 μM) or SCR (50 μM) for 1 h, separately, followed by stimulation with NMDA (100 μM) for 3 h, and the cells were stained with DAPI (Blue). The neuronal death ratios were plotted as average ± SEM (n = 3), *P < 0.05, ***P < 0.005 compared to control, ###P < 0.01, ####P < 0.005 compared to NMDA treatment. (i and j) Cortical neurons were pretreated with YEKL (50 μM) or SCR (50 μM) for 1 h, separately, followed by stimulation with NMDA (100 μM) for 3 h, the abundance of cleaved Caspase 3 was determined by Western blot. The cleaved Caspase 3/β-actin ratios were plotted as average ± SEM (n = 3), ***P < 0.005 compared to control, ###P < 0.01 compared to NMDA treatment. n.s.: not significant.

according to the endocytic YEKL motif, which mediated the binding of GluN2B and AP-2 to facilitate the Clathrin-mediated endocytosis of GluN2B. Moreover, we confirmed that our peptide has no effect on the interaction of GluN2B with PSD95, which exclude the possibility that our peptide acts in a similar way with Tat-NR2B9c.

It is still unknown how the endocytosis of NMDARs mediates NMDAR-dependent excitotoxicity. However, several researches have reported that endocytosis is a critical process involved in NMDAR signaling transduction. Neuronal activity-induced activation of PI3K/ATK pathway is mediated by Clathrin dependent endocytosis.^{39,40} Synaptic NMDAR-dependent transcription is also dependent on the endocytosis.⁴¹ Furthermore, it has been reported that clathrin adaptor protein β -arrestin interaction with activated c-Jun kinase during neuronal death, which provide a possibility that endocytic protein recruits pro-death molecules to endocytosed NMDARs and then mediates cell death.⁴²

NMDAR has been considered as a double edged sword in CNS. Simply blocking normal function of NMDAR leads to severe side effects such as memory loss or psychomimetic effects. Here, our finding that endocytosis of GluN2B is involved in NMDA-induced excitotoxicity provides a possibility to specifically abolish the pro-death effects of NMDAR, while leaving other function of NMDAR unaffected. In the future, the effect of peptide YEKL may be tested in animal models to confirm its role in protecting neurons from excitotoxicity.

Author contributions

YW performed the biochemical and immunostaining experiments; collected, analyzed, and interpreted the data; and participated in writing the paper. CWC and QY and MFJ performed the biochemical experiments; collected, analyzed, and interpreted the data. SQ was responsible for the overall supervision of the study; designed the experiments; analyzed and interpreted the data; and revised the paper.

Declaration of Conflicting Interests

The author(s) declared no potential conflicts of interest with respect to the research, authorship, and/or publication of this article.

Funding

The author(s) disclosed receipt of the following financial support for the research, authorship, and/or publication of this article: This work was supported by Grants National Natural Science Foundation of China (No. 81271453, 81471125 and 81671049) to S.Q, Zhejiang Science Fund for Distinguished Young Scholars (LR16C090001 to S.Q.) and the Fundamental Research Funds for the Central Universities of China.

References

1. Mony L, Kew JN, Gunthorpe MJ, et al. Allosteric modulators of NR2B-containing NMDA receptors: molecular mechanisms and therapeutic potential. *Br J Pharmacol* 2009; 157: 1301–1317.
2. Lau CG and Zukin RS. NMDA receptor trafficking in synaptic plasticity and neuropsychiatric disorders. *Nature Rev Neurosci* 2007; 8: 413–426.
3. Bliss TV and Collingridge GL. A synaptic model of memory: long-term potentiation in the hippocampus. *Nature* 1993; 361: 31–39.
4. Aamodt SM and Constantine-Paton M. The role of neural activity in synaptic development and its implications for adult brain function. *Adv Neurol* 1999; 79: 133–144.
5. Traynelis SF, Wollmuth LP, McBain CJ, et al. Glutamate receptor ion channels: structure, regulation, and function. *Pharmacol Rev* 2010; 62: 405–496.
6. Monyer H, Sprengel R, Schoepfer R, et al. Heteromeric NMDA receptors: molecular and functional distinction of subtypes. *Science* 1992; 256: 1217–1221.
7. Sheng M, Cummings J, Roldan LA, et al. Changing subunit composition of heteromeric NMDA receptors during development of rat cortex. *Nature* 1994; 368: 144–147.
8. Meguro H, Mori H, Araki K, et al. Functional characterization of a heteromeric NMDA receptor channel expressed from cloned cDNAs. *Nature* 1992; 357: 70–74.
9. Soriano FX, Martel MA, Papadia S, et al. Specific targeting of pro-death NMDA receptor signals with differing reliance on the NR2B PDZ ligand. *J Neurosci* 2008; 28: 10696–10710.
10. Borsello T, Croquelois K, Hornung JP, et al. N-methyl-D-aspartate-triggered neuronal death in organotypic hippocampal cultures is endocytic, autophagic and mediated by the c-Jun N-terminal kinase pathway. *Eur J Neurosci* 2003; 18: 473–485.
11. Kiselev A, Socolich M, Vinos J, et al. A molecular pathway for light-dependent photoreceptor apoptosis in *Drosophila*. *Neuron* 2000; 28: 139–152.
12. Alloway PG, Howard L and Dolph PJ. The formation of stable rhodopsin-arrestin complexes induces apoptosis and photoreceptor cell degeneration. *Neuron* 2000; 28: 129–138.
13. Malinow R and Malenka RC. AMPA receptor trafficking and synaptic plasticity. *Annu Rev Neurosci* 2002; 25: 103–126.
14. Man HY, Ju W, Ahmadian G, et al. Intracellular trafficking of AMPA receptors in synaptic plasticity. *Cell Mol Life Sci* 2000; 57: 1526–1534.
15. Wang Y, Ju W, Liu L, et al. alpha-Amino-3-hydroxy-5-methylisoxazole-4-propionic acid subtype glutamate receptor (AMPA) endocytosis is essential for N-methyl-D-aspartate-induced neuronal apoptosis. *J Biol Chem* 2004; 279: 41267–41270.
16. Wang YH, Bosy TZ, Yasuda RP, et al. Characterization of NMDA receptor subunit-specific antibodies: distribution of NR2A and NR2B receptor subunits in rat brain and ontogenic profile in the cerebellum. *J Neurochem* 1995; 65: 176–183.
17. Qiu S, Chen T, Koga K, et al. An increase in synaptic NMDA receptors in the insular cortex contributes to neuropathic pain. *Sci Signal* 2013; 6: ra34.

18. Qiu S, Zhang M, Liu Y, et al. GluA1 phosphorylation contributes to postsynaptic amplification of neuropathic pain in the insular cortex. *J Neurosci* 2014; 34: 13505–13515.
19. Choi DW. Excitotoxic cell death. *J Neurobiol* 1992; 23: 1261–1276.
20. Olney JW. Excitotoxicity, apoptosis and neuropsychiatric disorders. *Curr Opin Pharmacol* 2003; 3: 101–109.
21. Soriano SG, Coxon A, Wang YF, et al. Mice deficient in Mac-1 (CD11b/CD18) are less susceptible to cerebral ischemia/reperfusion injury. *Stroke* 1999; 30: 134–139.
22. Schmidt-Kastner R and Freund TF. Selective vulnerability of the hippocampus in brain ischemia. *Neuroscience* 1991; 40: 599–636.
23. Gao J, Duan B, Wang DG, et al. Coupling between NMDA receptor and acid-sensing ion channel contributes to ischemic neuronal death. *Neuron* 2005; 48: 635–646.
24. Liu Y, Wong TP, Aarts M, et al. NMDA receptor subunits have differential roles in mediating excitotoxic neuronal death both in vitro and in vivo. *J Neurosci* 2007; 27: 2846–2857.
25. Weilinger NL, Lohman AW, Rakai BD, et al. Metabotropic NMDA receptor signaling couples Src family kinases to pannexin-1 during excitotoxicity. *Nat Neurosci* 2016; 19: 432–442.
26. Dore K, Aow J and Malinow R. Agonist binding to the NMDA receptor drives movement of its cytoplasmic domain without ion flow. *Proc Natl Acad Sci U S A* 2015; 112: 14705–14710.
27. Nabavi S, Kessels HW, Alfonso S, et al. Metabotropic NMDA receptor function is required for NMDA receptor-dependent long-term depression. *Proc Natl Acad Sci U S A* 2013; 110: 4027–4032.
28. Stein IS, Gray JA and Zito K. Non-Ionotropic NMDA receptor signaling drives activity-induced dendritic spine shrinkage. *J Neurosci* 2015; 35: 12303–12308.
29. Chen N, Luo T and Raymond LA. Subtype-dependence of NMDA receptor channel open probability. *J Neurosci* 1999; 19: 6844–6854.
30. Vicini S, Wang JF, Li JH, et al. Functional and pharmacological differences between recombinant N-methyl-D-aspartate receptors. *J Neurophysiol* 1998; 79: 555–566.
31. Vaslin A, Puyal J, Borsello T, et al. Excitotoxicity-related endocytosis in cortical neurons. *J Neurochem* 2007; 102: 789–800.
32. Vaslin A, Puyal J and Clarke PG. Excitotoxicity-induced endocytosis confers drug targeting in cerebral ischemia. *Ann Neurol* 2009; 65: 337–347.
33. Rybin V, Ullrich O, Rubino M, et al. GTPase activity of Rab5 acts as a timer for endocytic membrane fusion. *Nature* 1996; 383: 266–269.
34. Lavezzari G, McCallum J, Lee R, et al. Differential binding of the AP-2 adaptor complex and PSD-95 to the C-terminus of the NMDA receptor subunit NR2B regulates surface expression. *Neuropharmacology* 2003; 45: 729–737.
35. Prybylowski K, Chang K, Sans N, et al. The synaptic localization of NR2B-containing NMDA receptors is controlled by interactions with PDZ proteins and AP-2. *Neuron* 2005; 47: 845–857.
36. Sattler R, Xiong Z, Lu WY, et al. Specific coupling of NMDA receptor activation to nitric oxide neurotoxicity by PSD-95 protein. *Science* 1999; 284: 1845–1848.
37. Aarts M, Liu Y, Liu L, et al. Treatment of ischemic brain damage by perturbing NMDA receptor- PSD-95 protein interactions. *Science* 2002; 298: 846–850.
38. Zhou L, Li F, Xu HB, et al. Treatment of cerebral ischemia by disrupting ischemia-induced interaction of nNOS with PSD-95. *Nat Med* 2010; 16: 1439–1443.
39. Luo HR, Hattori H, Hossain MA, et al. Akt as a mediator of cell death. *Proc Natl Acad Sci U S A* 2003; 100: 11712–11717.
40. Zheng J, Shen WH, Lu TJ, et al. Clathrin-dependent endocytosis is required for TrkB-dependent Akt-mediated neuronal protection and dendritic growth. *J Biol Chem* 2008; 283: 13280–13288.
41. Trifilieff P, Lavaur J, Pascoli V, et al. Endocytosis controls glutamate-induced nuclear accumulation of ERK. *Mol Cell Neurosci* 2009; 41: 325–336.
42. McDonald PH, Chow CW, Miller WE, et al. Beta-arrestin 2: a receptor-regulated MAPK scaffold for the activation of JNK3. *Science* 2000; 290: 1574–1577.